Acta Chemica Scandinavica, 1999: 53: 876–886
Printed in UK. All rights reserved

ACTA
CHEMICA SCANDINAVICA
ISSN 0904-213X

Two-Electron-Transfer Redox Systems. Part 3.† Electrochemical Reduction of *N,N'*-Dialkyl-4,5-dimethylimidazolium-2-dithiocarboxylates to 1,1-Dithiolate Dianions in THF. Steric Modulation of Potential Ordering by Substituents

Stefan Dümmling,[a] Bernd Speiser,*[,a] Norbert Kuhn[b] and Gerd Weyers[b]

[a]Institut für Organische Chemie, Auf der Morgenstelle 18, D-72076 Tübingen, Germany and [b]Institut für Anorganische Chemie, Auf der Morgenstelle 18, D-72076 Tübingen, Germany

Dedicated to Professor Henning Lund on the occasion of his 70th birthday.

Dümmling, S., Speiser, B., Kuhn, N. and Weyers, G., 1999. Two-Electron-Transfer Redox Systems. Part 3. Electrochemical Reduction of *N,N'*-Dialkyl-4,5-dimethylimidazolium-2-dithiocarboxylates to 1,1-Dithiolate Dianions in THF. Steric Modulation of Potential Ordering by Substituents. – Acta Chem. Scand. 53: 876–886. © Acta Chemica Scandinavica 1999.

Three CS_2 adducts of imidazol-2-ylidenes, *N,N'*-dialkyl-4,5-dimethylimidazolium-2-dithiocarboxylates (alkyl = CH_3, C_2H_5, i-C_3H_7), have been reduced electrochemically at a glassy carbon electrode in THF. For the methyl and the ethyl compounds two reduction peaks are observed in their cyclic voltammograms, while the isopropyl derivative exhibits a single signal. Chronocoulometric results and numerical simulations show that the formal potentials for the two electron transfer steps are 'compressed', and in the isopropyl case even 'inverted'. This behavior is due to a steric interaction between the alkyl substituents and the semi-occupied orbital in the respective monoanion. It is consistent with the fact that during the two-electron reduction a considerable structural change occurs, most likely during the second electron-transfer step.

The transfer of a single electron to (reduction) or from a molecule (oxidation) is described in detail by the Marcus theory.[2–5] Such an electron transfer may be induced thermally (by chemical reaction), photochemically, or electrochemically. Besides being important for the generation of persistent, intermediate, or reactive species in unusual oxidation states, single-electron transfer reactions have been discussed in the context of substitutions such as $S_{RN}1$ or S_N2 reactions,[6,7] and they take part in important biological processes, such as photosynthesis.[8] Much less work has been devoted to the understanding of multiple redox systems,[9] where more than one electron is transferred. Such reactions have been identified in inorganic redox systems [e.g., Tl(I/III)[10]], organometallic complexes [e.g., bis(hexamethylbenzene)ruthenium(II/0)[11,12]], and in organic compounds (for some earlier examples, see Refs. 9, 13). Again, natural (nitrogen fixation[14]) and technical processes (catalysis,[15] fuel cells[16]) are based on multi-electron transfers.

The most simple model of such reactions is to assume a stepwise transfer of the electrons, either with separate reaction intermediates ('conventional') or within a single collision complex ('unconventional' stepwise mechanism).[17] If the thermodynamics are favourable (see below) and the rates of the second and further electron transfers are extremely fast, making the intermediate(s) unstable, one could regard the transfers as being simultaneous.[18] It has, however, recently been noted, and elaborated on a theoretical basis, that multi-electron transfers may be concerted[17,19] or, even more complex, co-operative, self-organized, or synergetic.[16,20,21]

We will retain the simple stepwise description in the present paper. However, even under such an assumption, already *two*-electron-transfer redox systems may show a much broader variety of behavior than is observed for one-electron processes. Heinze has thus denoted the electrochemical two-electron-transfer EE mechanism as 'many-faceted'.[22]

† Part 2: see Ref. 1.

* To whom correspondence should be addressed: fax: +49-7071-295518, e-mail: bernd.speiser@uni-tuebingen.de

In Scheme 1 such a stepwise two-electron-transfer redox system is formulated for the redox-active species A^0, $A^{1+/-}$, and $A^{2+/-}$, where the superscript indicates the difference of the redox states relative to the starting species A^0 (here assumed to be chemically stable under the conditions of the experiments). Although A^0 is neutral in the case investigated in the present paper, the starting species may in general also be charged. The positive sign in the superscripts refers to an oxidation process, the negative one to a reduction (to be discussed here). The primary electron transfer products may undergo chemical follow-up reactions to products, P and P', respectively. It is important to note that there exists an additional disproportionation–comproportionation equilibrium between the three redox species which is also shown in Scheme 1.

The thermodynamics of a two-electron-transfer redox system is determined by the respective formal potentials E_1° and E_2° of the two one-electron processes. In many cases species become more difficult to oxidize with increasing oxidation state, or, on the other hand, more difficult to reduce with decreasing oxidation state. Thus, the formal potential difference

$$|\Delta E^\circ| = \begin{cases} E_2^\circ - E_1^\circ & \text{for an oxidation} \\ -(E_2^\circ - E_1^\circ) & \text{for a reduction} \end{cases} \quad (1)$$

is positive ('normal potential ordering').

From purely electrostatic considerations, one would expect *in vacuo* a value[13] of $|\Delta E^\circ| \approx 5$ V. For aprotic solvents, however, it has been shown that due to solvation effects, $|\Delta E^\circ|$ decreases to several tenths of a volt, often attaining values in the range[13] 0.4–0.5 V. A large variety of chemical compounds has been characterized which indeed conform to this rule.

The value of $|\Delta E^\circ|$ determines the value of the comproportionation equilibrium constant, eqn. (2).

$$K_{comp} = \frac{[A^{1+/-}]^2}{[A^0][A^{2+/-}]} = \exp\left[\frac{F}{RT}|\Delta E^\circ|\right] \quad (2)$$

In the case of normal potential ordering, K_{comp} is larger than unity and the intermediate redox state, $A^{1+/-}$, is stable with respect to disproportionation. However, several examples have been discussed (see, e.g. Refs. 18, 23, 24 and references therein), where $|\Delta E^\circ|$ is 'compressed' to values much smaller than ≈ 0.4 V, or even attains negative values ('inverted potential ordering'). In the latter case, $A^{1+/-}$ becomes unstable with respect to disproportionation ($K_{comp} < 1$) and will homogeneously react in solution to A^0 and $A^{2+/-}$.

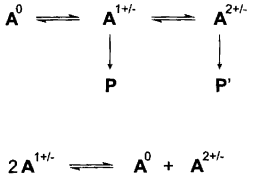

Scheme 1.

Concomitant with potential inversion, one often observes a considerable change in the structure of the redox-active species, for example conformational changes,[12] or changes in cluster geometry.[25] Such 'inner reorganization' of the molecule[3] leads to a decrease in the electron transfer rate constant. Additionally, in electrochemical experiments, a 'kinetic burden of potential inversion'[18] has been identified which is related to the potential dependence of the electron transfer rate.

In order to identify the prerequisites for the occurrence of potential inversion, it seems desirable to characterize chemical systems, in which the variation of substituents allows fine-tuning of various structural aspects of the molecules. In the present paper we report on the redox properties of a series of three *N,N'*-dialkyl-substituted 4,5-dimethylimidazolium-2-dithiocarboxylates **1a–c**. In these molecules we are able to modulate potential ordering for the two-electron reduction from normal to inverted by the steric demand of the alkyl substituents.

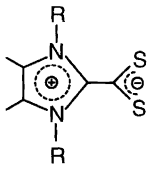

1 **a** R = CH_3
b R = C_2H_5
c R = i-C_3H_7

Both thermodynamics and kinetics of electrochemical redox processes can easily be followed by cyclic voltammetry. Therefore, this technique was mainly used in the present work. Data from cyclic voltammetry were complemented with those from chronocoulometry.

Results and discussion

Cyclic voltammetry. The meso-ionic dithiocarboxylates **1a–c** are soluble in only a few solvents. Of these only THF has an accessible potential window with a lower limit of -3 V which is sufficiently negative to allow investigation of the electrochemical reduction of the electron-rich compounds. A disadvantage of THF electrolytes is their high resistance (in our experiments in the range 2.2–2.5 kΩ for a distance of ≈1–2 mm between the working electrode and the Haber–Luggin tip). The resulting large *iR*-drop limits cyclic voltammetry to maximum scan rates of $v = 2$ V s^{-1} at concentrations in the 0.1–1 mM range and planar electrodes with a diameter of ≈3 mm. At higher scan rates satisfactory *iR* compensation was not possible. Scan rates below $v = 0.05$ V s^{-1} did not give reproducible results and the cyclic voltammetric curves showed artefacts probably caused by convection in the solution.

A series of cyclic voltammetric experiments performed with ferrocene (fc) in THF (three different concentrations) under identical experimental conditions showed

the same limitations as found with **1a–c**. Consequently, experiments with the dithiocarboxylates were restricted to scan rates $v = 0.05$–$2.0\ V\ s^{-1}$.

Cyclic voltammograms of the methyl compound **1a** showed up to four peaks (Fig. 1; circles). Individual peak potentials (E_p^I, E_p^{II}, E_p^{III}, E_p^{IV}; for the numbering of peaks, see Fig. 1a) are essentially independent of the concentration (Table 1). Hence, the *iR* drop in the electrolyte was effectively compensated. Furthermore, reactions of an order higher than unity do not significantly affect the results. On the other hand, the peak potentials shift with v. At slow v, the peak potential differences ΔE_p for both reduction processes are not much different and close to the reversible limit of 58 mV for a one-electron process (Table 1). Their values are independent of c, but increase with v. The ΔE_p of the peak couple at more negative potentials (peaks II and III) grows faster than that of the peak couple at less negative potentials (peaks I and IV). This indicates that **1a** is electrochemically reduced in two quasi-reversible one-electron transfer steps, the first one being faster than the second one. The mid-point potentials (mean values of the corresponding cathodic and anodic peak potentials; values in Table 1) are independent of v and c with mean values over all c and v of $\bar{E}^{I/IV} = (-2.308 \pm 0.001)\ V$ and $\bar{E}^{II/III} = (-2.476 \pm 0.003)\ V$.

Of the peak currents in the voltammograms of **1a** only i_p^I is meaningful, since the small separation of the signals does not allow simple determination of the baselines for the other i_p. For the same reason, peak current ratios were not interpreted. Analysis of the data for i_p^I (Table 1) showed that this peak current is essentially proportional to $v^{1/2}$ and c.

Cyclic voltammograms of the *N,N'*-diethyl derivative **1b** (Fig. 2) showed that the replacement of the two methyl groups in **1a** by two ethyl groups causes a shift of both reduction waves to more negative potentials [$\bar{E}^{I/IV} = (-2.364 \pm 0.002)\ V$, $\bar{E}^{II/III} = (-2.496 \pm 0.005)\ V$ (only $v = 0.05\ V\ s^{-1}$, two c)]. Since the two reduction processes are affected differently, the peaks in the cyclic voltammograms of **1b** are spaced more closely than those in the current–potential curves of **1a**. Furthermore,

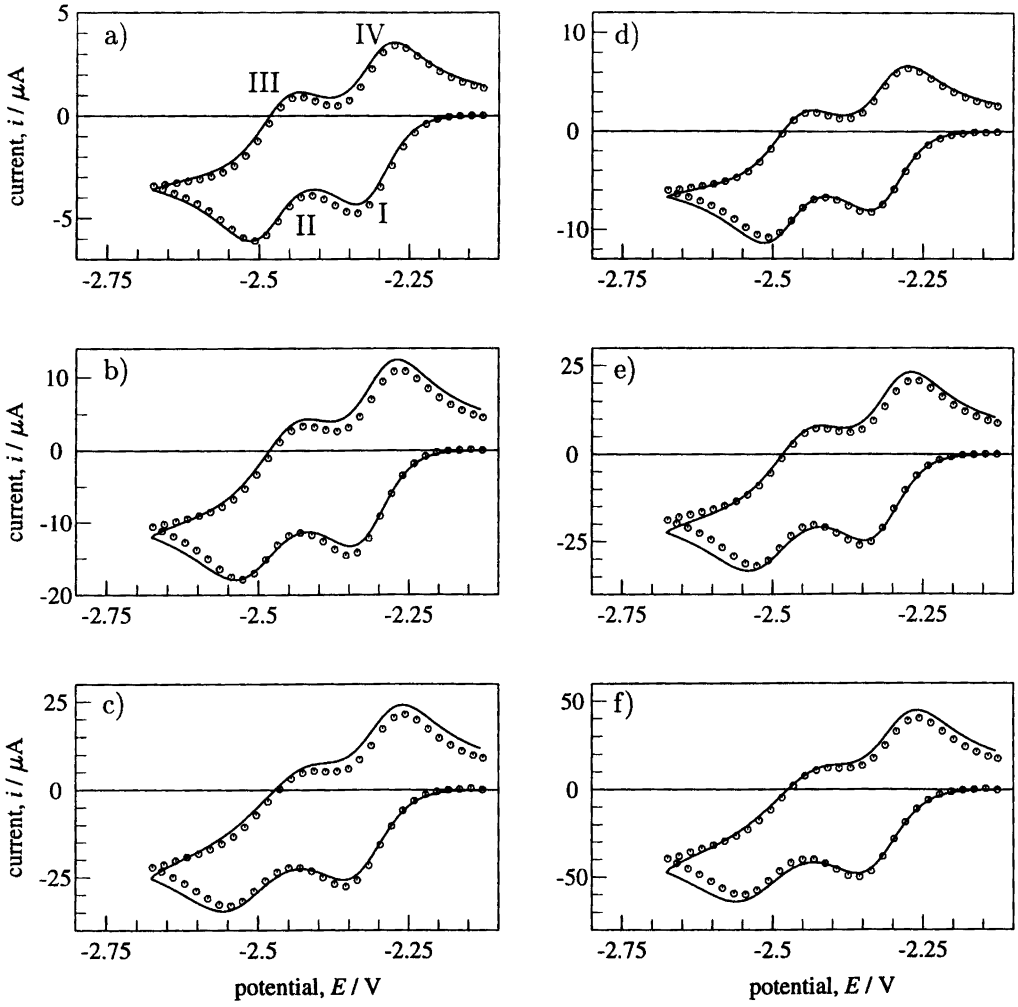

Fig. 1. Cyclic voltammograms of **1a** in THF–0.2 NBu_4PF_6 at a GC electrode: circles, experimental data; lines, simulations (for parameters see the text and Table 4); (a)–(c) $c = 0.36$ mM; (d)–(f) $c = 0.67$ mM; (a), (d) $v = 0.05\ V\ s^{-1}$; (b), (e) $v = 0.5\ V\ s^{-1}$; (c), (f) $v = 2.0\ V\ s^{-1}$.

Table 1. Potential[a] and current[b] results from cyclic voltammograms[c] of **1a**.

c/mM	v/V s^{-1}	E_p^I/V	E_p^{II}/V	E_p^{III}/V	E_p^{IV}/V	$\Delta E_p^{I/IV}$/V	$\Delta E_p^{II/III}$/V	$\bar{E}^{I/IV}$/V	$\bar{E}^{II/III}$/V	i_p^I/μA
0.36	0.05	−2.341	−2.509	−2.434	−2.272	0.069	0.075	−2.307	−2.472	4.79
0.36	0.1	−2.343	−2.514	−2.433	−2.271	0.072	0.081	−2.307	−2.474	6.63
0.36	0.2	−2.345	−2.520	−2.432	−2.269	0.076	0.088	−2.307	−2.476	9.34
0.36	0.5	−2.350	−2.531	−2.423	−2.265	0.085	0.108	−2.308	−2.477	14.6
0.36	1.0	−2.356	−2.540	−2.417	−2.261	0.095	0.123	−2.309	−2.479	19.9
0.36	2.0	−2.359	−2.551	−2.409	−2.258	0.101	0.142	−2.309	−2.480	27.7
0.67	0.05	−2.342	−2.510	−2.436	−2.275	0.067	0.074	−2.309	−2.473	8.30
0.67	0.1	−2.345	−2.515	−2.430	−2.271	0.074	0.085	−2.308	−2.473	11.6
0.67	0.2	−2.348	−2.520	−2.427	−2.269	0.079	0.093	−2.309	−2.474	16.4
0.67	0.5	−2.352	−2.529	−2.420	−2.264	0.088	0.109	−2.308	−2.475	26.1
0.67	1.0	−2.355	−2.539	−2.416	−2.263	0.092	0.123	−2.309	−2.478	35.8
0.67	2.0	−2.361	−2.551	−2.401	−2.260	0.101	0.150	−2.311	−2.476	50.1

[a]Referred to fc/fc$^+$ in THF. [b]Referred to zero current. [c]Peak numbering see Fig. 1a.

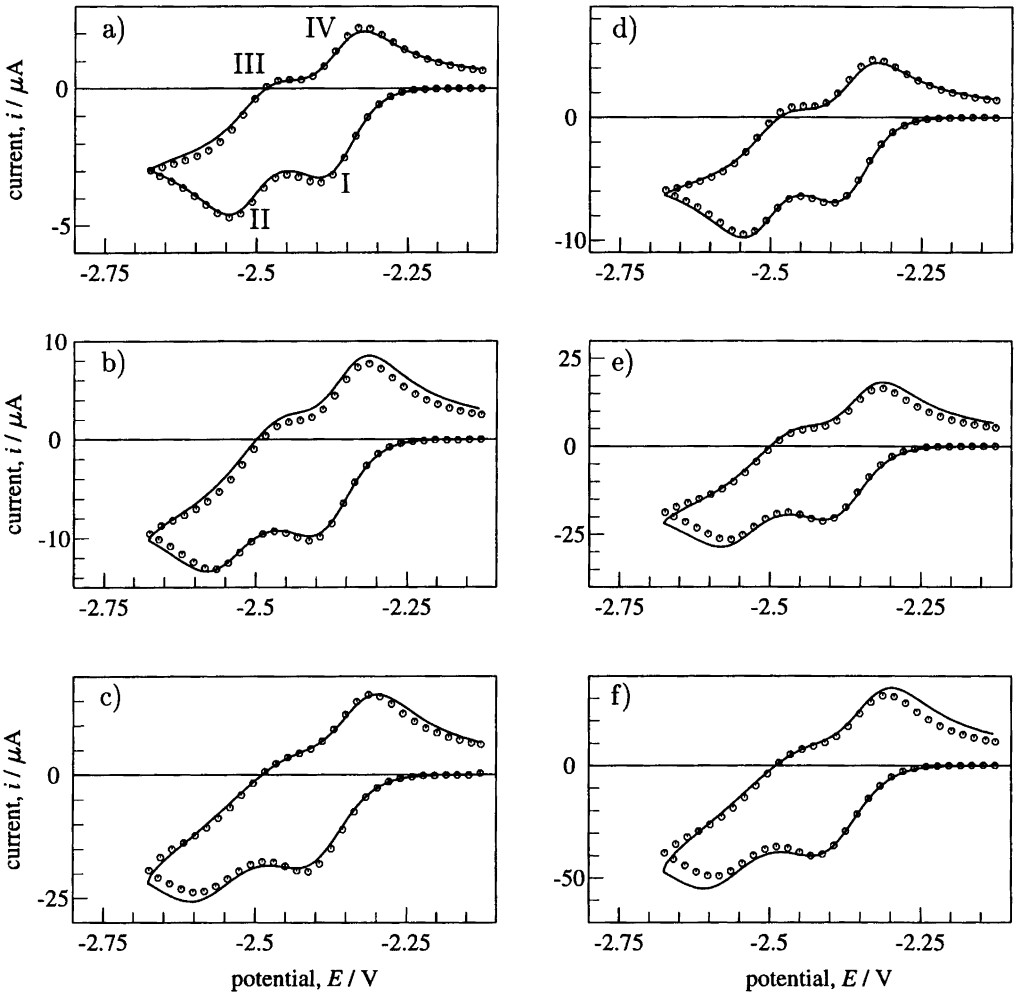

Fig. 2. Cyclic voltammograms of **1b** in THF–0.2 NBu_4PF_6 at a GC electrode: circles, experimental data; lines, simulations (for parameters see the text and Table 4); (a)–(c) c=0.23 mM; (d)–(f) c=0.49 mM; (a), (d) v=0.05 V s^{-1}; (b), (e) v=0.5 V s^{-1}; (c), (f) v=2.0 V s^{-1}.

peak III is no longer clearly separated from peak IV at scan rates above v=0.05 V s^{-1}. For v=0.05 V s^{-1} a value of $|\Delta E^\circ| \approx 0.130$ V is found. The ΔE_p values of the first peak couple exhibit the same characteristics as those of **1a**, but are approximately 0.01 V larger. For the second peak couple ΔE_p could only be estimated for the slowest scan rate ($\Delta E_p^{II/III} \approx 0.100$ V).

From the analysis of the cyclic voltammograms of **1a** and **1b** we concluded that these compounds are reduced in two steps to mono- and di-anions, $\mathbf{1}^{\cdot -}$ and $\mathbf{1}^{2-}$,

respectively. This is in accordance with the chemical reduction of **1b** with potassium metal in THF,[26] which leads to $\mathbf{1b}^{2-}2K^{+}$. Under the assumption of equal diffusion coefficients for the redox species involved, $\bar{E}$ from the experiments are regarded as good approximations to the formal potentials E_1° ($\mathbf{1a}+e^- \rightleftharpoons \mathbf{1a}^{\cdot -}$) and E_2° ($\mathbf{1a}^{\cdot -}+e^- \rightleftharpoons \mathbf{1a}^{2-}$).

The isopropyl derivative **1c** showed cyclic voltammograms that displayed only *one* reduction and *one* oxidation peak for all concentrations and scan rates (Fig. 3, circles). The values (see Table 2) of the mid-point potential, the peak potential difference, the peak current ratio (i_p^{II}/i_p^{I}) and the peak current function ($i_p^{I} v^{-1/2} c^{-1}$) were independent of the concentration. The $\bar{E}^{I/II}$ values were independent of v [mean value over all v and c: (-2.448 ± 0.001) V]. As for **1a** and **1b**, however, significant variations of the other voltammetric features with v were observed. In particular, the peak potential difference increased with v, while the peak current function decreased slightly (quasi-reversibility). The peak current ratio was smaller than unity, indicating the possible interference of a chemical follow-up reaction. As for **1b**, the chemical reduction of **1c** with K in THF led to a dianion $\mathbf{1c}^{2-}$ (X-ray analysis of the product[27]). This result suggests that although only a single reduction peak is observed for **1c**, under electrochemical conditions a two-electron process also occurs. This is substantiated by chronocoulometric experiments and numerical simulations below.

Chronocoulometry. Double step chronocoulometric experiments were employed at potentials sufficiently negative of the voltammetric peaks to enable diffusion-controlled reduction of the dithiocarboxylates **1**. A series of chronocoulometric experiments was performed with fc to test the limitations under our experimental conditions. Only for pulse widths $0.5\,s \leqslant \tau \leqslant 5\,s$ were constant slopes in the plots of Q vs. $t^{1/2}$ (forward step) or vs. $\theta = \tau^{1/2} + (t-\tau)^{1/2} - t^{1/2}$ (reverse step) ('Anson plots')[28] and a constant $Q_{2\tau}/Q_\tau$ ratio of 0.44 ± 0.01 (Q_τ: charge transferred at the end of forward step with pulse width τ; $Q_{2\tau}$: charge transferred at the end of the reverse step)

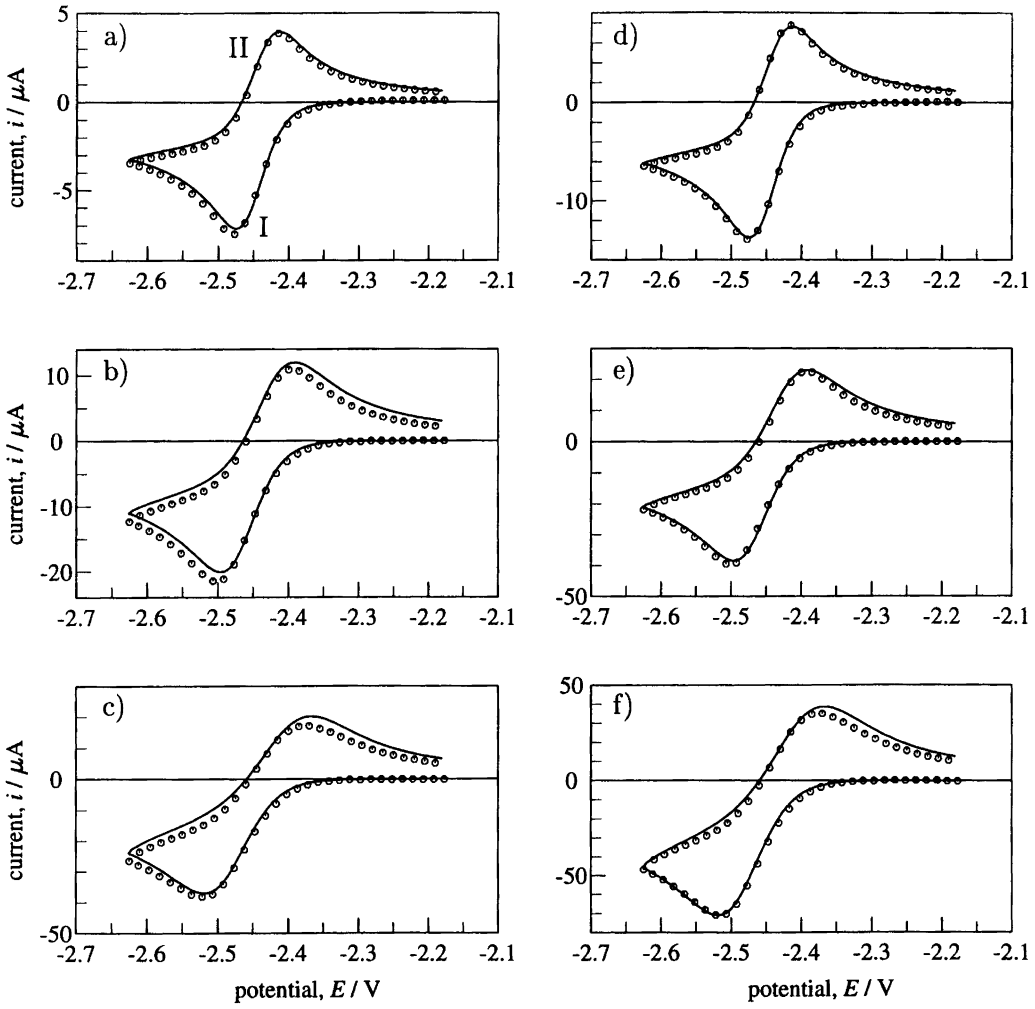

Fig. 3. Cyclic voltammograms of **1c** in THF–0.2 NBu_4PF_6 at a GC electrode: circles, experimental data; lines, simulations (for parameters see the text and Table 4); (a)–(c) $c = 0.24$ mM; (d)–(f) $c = 0.46$ mM; (a), (d) $v = 0.05\ V\,s^{-1}$; (b), (e) $v = 0.5\ V\,s^{-1}$; (c), (f) $v = 2.0\ V\,s^{-1}$.

Table 2. Potential[a] and current[b] results from cyclic voltammograms[c] of **1c**.

c/mM	v/V s^{-1}	E_p^I/V	E_p^{II}/V	ΔE_p/V	$\bar{E}^{I/II}$/V	i_p^I/μA	i_p^{II}/μA	i_p^{II}/i_p^I	$i_p^I v^{-1/2} c^{-1}$ [d]
0.24	0.05	−2.478	−2.415	0.063	−2.447	7.49	3.89	0.83	137
0.24	0.1	−2.482	−2.413	0.069	−2.448	10.3	5.49	0.85	134
0.24	0.2	−2.493	−2.405	0.088	−2.449	14.2	7.52	0.87	130
0.24	0.5	−2.501	−2.395	0.106	−2.448	21.5	11.0	0.87	125
0.24	1.0	−2.507	−2.390	0.117	−2.449	29.1	14.0	0.87	119
0.24	2.0	−2.522	−2.376	0.146	−2.449	38.2	17.2	0.87	111
0.46	0.05	−2.476	−2.416	0.060	−2.446	13.9	7.74	0.87	135
0.46	0.1	−2.482	−2.411	0.071	−2.447	19.0	11.2	0.91	130
0.46	0.2	−2.489	−2.403	0.086	−2.446	26.1	15.5	0.92	126
0.46	0.5	−2.501	−2.393	0.108	−2.447	39.8	22.6	0.92	121
0.46	1.0	−2.510	−2.386	0.124	−2.448	52.5	27.9	0.91	113
0.46	2.0	−2.516	−2.376	0.140	−2.446	71.0	35.2	0.90	108

[a]Referred to fc/fc$^+$ in THF. [b]Referred to zero current; [c]Peak numbering see Fig. 3a. [d]In A V$^{-1/2}$ s$^{1/2}$ mol^{-1} cm^3.

found close to the theoretical value of 0.414 for systems without follow-up reaction.[29] Hence, chronocoulometric experiments with the dithiocarboxylates were only performed within this timescale (for typical curves for **1c** see Fig. 4; for results see Table 3).

The Anson plots (see Fig. 4a for the example of **1c**) show that none of the compounds is adsorbed at the glassy carbon electrode surface (intercept with Q axis after background correction essentially zero, intersection of lines at $Q=0$ axis).[30] Slopes of the forward traces in the Anson plots of **1a–c** were constant for various τ for a particular compound. From the Anson plot slopes the diffusion coefficients D of the neutral species were calculated (Table 3) under the assumption of a net two-electron reduction, $n=2$. The number of transferred electrons could clearly be inferred for the reduction of **1a** and **1b** from the cyclic voltammograms of the respective dithiocarboxylate. The analysis of the chronocoulometric data for the reduction of **1c**, however, was tested for both $n=1$ and $n=2$. With $n=1$, from the Anson plot slope a diffusion coefficient $D(\mathbf{1c}) = (60\pm4)\times10^{-6}$ cm^2 s^{-1} would follow, which is about 4 to 5 times larger than that of $D(\mathbf{1a})$ and $D(\mathbf{1b})$. Such a result is highly improbable, considering the molecular masses of the three dithiocarboxylates investigated which differ by only about 25%. On the other hand, with $n=2$ a reasonable $D(\mathbf{1c})$ could be calculated (Table 3). Thus, in accordance with the results for **1a** and **1b**, as well as the chemical reduction experiments,[26,27] we conclude that the isopropyl derivative **1c** is also electrochemically reduced to a dianion. This conclusion is further confirmed by numerical simulations (see below). The fact that the cyclic voltammogram of **1c** does show only a single reduction peak I (Fig. 3) has then to be explained by strong 'compression' or even 'inversion' of the formal potentials for the two reduction steps.

Values of the ratio $Q_{2\tau}/Q_\tau$ for **1a–c** lie between 0.47 and 0.61 and are essentially independent of the concentration. They increase slightly with increasing τ. These features indicate a slow follow-up reaction of (pseudo-)first-order of either the dianion and/or the monoanion. The influence of this follow-up reaction can also be seen in the Anson plots (Fig. 4a). For an uncomplicated electron transfer without follow-up reaction and without adsorption, one expects a straight line for the trace of the reverse step and identical absolute values for the slopes of the forward and the reverse trace. In our cases, the reverse traces are slightly bent, as would be expected from the theory of chronocoulometry for electrode reactions involving follow-up steps.[31] The absolute

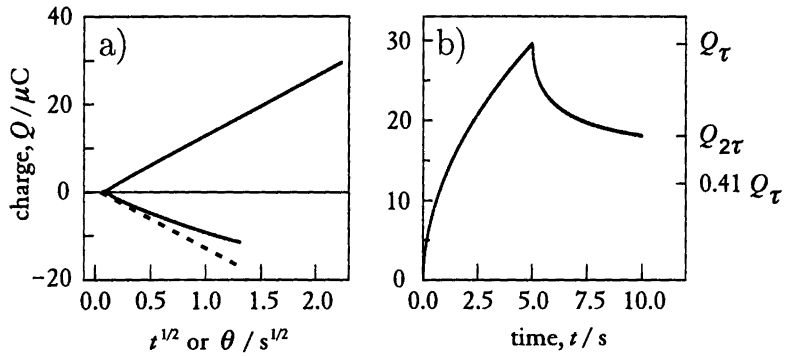

Fig. 4. Chronocoulometric results for **1c**: (a) solid lines: Anson plot for the chronocoulogram in (b); broken line: theoretical plot for reduction in the absence of adsorption and follow-up reaction. The horizontal axis is $t^{1/2}$ for the forward step (upper trace) and $\theta=\tau^{1/2}+(t-\tau)^{1/2}-t^{1/2}$ for the reverse step (lower trace); (b) chronocoulogram in THF–0.2 NBu_4PF_6 at a GC electrode, $c=0.24$ mM, $\tau=5$ s.

Table 3. Results from chronocoulograms of **1a–c**.

τ/s	c/mM	$Q_{2\tau}/Q_\tau$	$D/10^{-6}$ cm^2 s^{-1}
1a			
0.5	0.36	0.51	9.9
1	0.36	0.51	9.8
2	0.36	0.51	9.5
5	0.36	0.52	9.7
0.5	0.67	0.48	9.3
1	0.67	0.47	8.8
2	0.67	0.48	8.7
5	0.67	0.49	9.0
Mean value:			9.3±0.4
1b			
0.5	0.23	0.52	14.0
1	0.23	0.53	13.9
2	0.23	0.56	14.8
5	0.23	0.61	16.0
0.5	0.49	0.49	12.6
1	0.49	0.50	12.3
2	0.49	0.52	12.4
5	0.49	0.55	12.9
Mean value:			14±1
1c			
0.5	0.24	0.57	17.2
1	0.24	0.57	16.6
2	0.24	0.58	16.1
5	0.24	0.61	16.2
0.5	0.46	0.52	14.7
1	0.46	0.52	14.2
2	0.46	0.53	13.9
5	0.46	0.56	13.8
Mean value:			15±1

values of the limiting slopes of the reverse traces at small θ (broken line in Fig. 4a) are essentially identical with the slopes of the forward traces, further confirming the absence of adsorption.[30]

Numerical simulations. Cyclic voltammograms of the dithiocarboxylates **1** were numerically simulated under the assumption of two quasi-reversible electron transfers (E) and a homogeneous first-order irreversible follow-up chemical reaction (C) of the dianion (EEC mechanism) under linear diffusion conditions, with and without a coupled disproportionation–comproportionation equilibrium. Various combinations of parameter values were tested, and, also, alternative mechanisms were used.

In all cases good agreement between experimental and simulated curves for the entire range of c and v could be obtained only using the EEC mechanism. All attempts to fit the cyclic voltammograms of **1c** with a single electron transfer mechanism (E, EC) failed. Earlier, preliminary results for the reduction mechanism of **1c** (ECEC reaction)[26] were probably influenced by the presence of electroactive impurities.

Numerical values of the system parameters (formal potentials E_1° and E_2° for the two redox processes, heterogeneous electron transfer rate constants k_{s1} and k_{s2}, the diffusion coefficients D, as well as rate constants for the homogeneous comproportionation, k_{comp}, and for the follow-up reaction of the $\mathbf{1}^{2-}$, k_1) were taken from optimal simulations of the experimental curves.

The experimental data in Figs. 1–3 (circles) are superimposed with such optimal simulations (lines) for two concentrations and three selected scan rates. The parameters used for these calculations are listed in Table 4. The formal potentials compare extremely well with the mid-point potentials derived from the analysis of the cyclic voltammetric curves in the cases of **1a** and **1b**. The optimal k_s values confirm that the second electron transfer is slower than the first for all three **1**, as already seen from the qualitative analysis of the voltammograms. The transfer coefficients α_1 and α_2 were both set to 0.5. Variation of the latter parameters did not improve the fitting in any case.

On the other hand, variation of the diffusion coefficients under the simplifying assumption that the D of all species in the respective system $\mathbf{1}/\mathbf{1}^{\cdot-}/\mathbf{1}^{2-}$ are equal resulted in slightly better agreement. Still, the optimal D-values for the simulations did not differ much from the experimental values found from chronocoulometry (compare values in Tables 3 and 4).

The possible influence of the comproportionation equi-

Table 4. System parameters for simulation of cyclic voltammograms of dithiocarboxylates **1**.

Reaction step	System parameter(s)	**1a**	**1b**	**1c**
$\mathbf{1}+e^- \rightleftharpoons \mathbf{1}^{\cdot-}$	E_1°/V	−2.306	−2.357	−2.459
	k_{s1}/cm s^{-1}	0.029	0.0186	0.027
	α_1	0.5	0.5	0.5
$\mathbf{1}^{\cdot-}+e^- \rightleftharpoons \mathbf{1}^{2-}$	E_2°/V	−2.475	−2.502	−2.428
	k_{s2}/cm s^{-1}	0.009	0.0075	0.011
	α_2	0.5	0.5	0.5
$\mathbf{1}+\mathbf{1}^{2-} \rightleftharpoons 2\,\mathbf{1}^{\cdot-}$	K_{comp}	718.1	282.2	—
	k_{comp}/M^{-1} s^{-1}	2.7×10^5	1.45×10^6	—
$\mathbf{1}^{2-} \rightarrow$ product(s)	k_1/s^{-1}	0.07	0.25	0.045
	$D/10^{-6}$ cm^2 s^{-1}[a]	10.0	13.5	12.0

[a]All diffusion coefficients $D(\mathbf{1})$, $D(\mathbf{1}^{\cdot-})$, $D(\mathbf{1}^{2-})$ and D(product) for a particular compound were assumed to be equal.

librium (Scheme 1) on the simulated voltammograms was investigated by variation of the rate constant k_{comp}. In general, cyclic voltammograms of two-electron processes are only affected by such a homogeneous reaction, if at least one of the two heterogeneous electron transfers is slow. The influence of the homogeneous reaction increases with increasing differences between the redox potentials and between the heterogeneous rate constants k_{s1} and k_{s2} [for detailed discussions, see Refs. 32–34]. This was confirmed in the numerical simulations for the present cases by varying k_{comp} between 0 and $10^{12}\,M^{-1}\,s^{-1}$. At high scan rates and with $k_{comp} > 10^4\,M^{-1}\,s^{-1}$, the comproportionation affected the cyclic voltammograms of **1a** and **1b** significantly (see Fig. 5 for the example of **1b**). In particular, the shape of the current–potential curve on the reverse scan and in the region of peak III (arrow in Fig. 5b) could only be modelled adequately when the comproportionation reaction was taken into account. At low scan rates, variation of k_{comp} also influenced the reverse scans of the voltammograms, but these effects could be balanced out by changing k_1 (see below). Optimal values for k_{comp} indicated a fast, but not diffusion-controlled reaction. The value of K_{comp}, the comproportionation equilibrium constant, was calculated by DigiSim internally from $|\Delta E^\circ|$ ['thermodynamically superfluous reaction',[35] see eqn. (2)] and could not be changed.

In the case of **1c**, the fitting could not be improved by setting $k_{comp} \neq 0$. Consequently, the homogeneous redox reaction was not included into the simulations of the current–potential curves of the isopropyl compound.

The influence of the follow-up C-step on the fitting is significant only for $v = 0.05$ and $0.1\ V\,s^{-1}$ and vanishes for scan rates above $0.1\ V\,s^{-1}$. As the chronocoulometric and cyclic voltammetric results are independent of the substrate concentration, the chemical reaction of the dianions $\mathbf{1}^{2-}$ was formulated as being first-order in the simulations. DigiSim does not allow totally irreversible chemical reactions to be modelled directly. Such a condition was approximated, however, by choosing a very high value ($K_1 = 10^8$) for the equilibrium constant of the follow-up reaction. Optimal values for the k_1 are given in Table 4.

The numerical simulations thus confirm the qualitative and quantitative analyses of the cyclic voltammograms and chronocoulograms.

Thermodynamics and kinetics of imidazolium-2-dithiocarboxylate reduction. The formal potentials E° determined for the two reduction steps of the dithiocarboxylates **1** and the mean values of the respective E°, $\overline{E^\circ} = (E_0^1 + E_0^2)/2$ depend on the substituents R at the heterocyclic nitrogen atoms (Fig. 6). Values of $\overline{E^\circ}$ represent the energetics of the overall two-electron reduction process. Their shift [$\overline{E^\circ}$(**1a**) = −2.391 V, $\overline{E^\circ}$(**1b**) = −2.430 V and $\overline{E^\circ}$(**1c**) = −2.444 V] is explained by the $+I$-effect of the alkyl substituents: the slightly increasing electron donating abilities of the higher R makes the imidazolium-2-dithiocarboxylates increasingly difficult to reduce. In accordance with the relatively small differences in the $+I$ effect of CH_3, C_2H_5, and i-C_3H_7, however, the thermodynamic effect is only a few tens of mV.

Figure 6 also demonstrates the influence of the substituents on the relative formal potentials of the two one-electron transfers: whereas the reductions of **1a** and **1b** follow the normal ordering of potentials ($|\Delta E^\circ| > 0$) which are already 'compressed' compared with many other cases, the potentials for the reduction of **1c** are indeed 'inverted' ($|\Delta E^\circ| < 0$).

We explain the occurrence of compressed/inverted potentials in the case of the dithiocarboxylates **1** as due

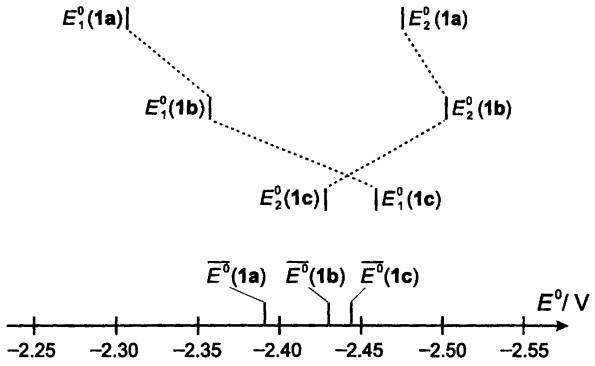

Fig. 6. Variation of formal potentials E_1° and E_2° (from simulations) as well as overall two-electron potentials $\overline{E^\circ}$ for reduction of dithiocarboxylates **1**.

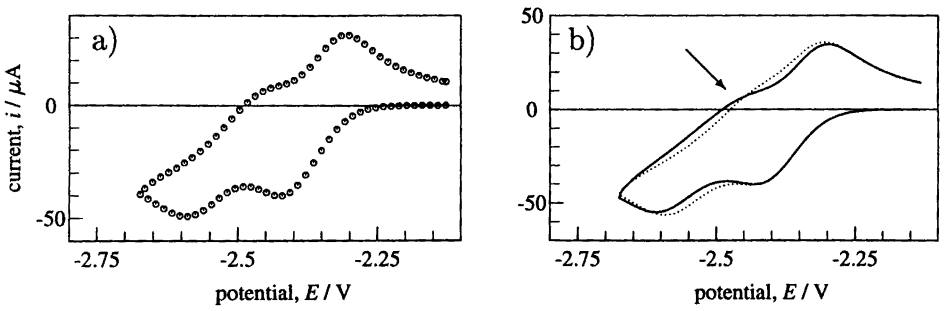

Fig. 5. Experimental (a) and simulated (b) voltammograms of **1b**, $v = 2.0\ V\,s^{-1}$, $c = 0.49$ mM; (b) without ($k_{comp} = 0\ M^{-1}\,s^{-1}$; dotted line) and with homogeneous comproportionation reaction ($k_{comp} = 1.45 \times 10^6\ M^{-1}\,s^{-1}$; full line).

to structural changes accompanying the reduction process. A comparison of the X-ray structures of **1b**[36] and the dipotassium salt[27] of $\mathbf{1c}^{2-}$ as well as a consideration of the NMR spectroscopic properties of the neutral compounds and their dianions[26,27,36] reveals that the chemical reduction of the dithiocarboxylates with potassium in THF is accompanied by a rotation of the CS_2 fragment from being orthogonal to the imidazole ring to a geometry where the molecule is planar and exhibits an exocyclic C=C double bond. We assume that the same geometrical changes occur during the electrochemical reduction (Fig. 7). Without such a rotation, the second electron transfer would result in an obviously energetically unfavorable diradical ($\mathbf{1}^{2-}_{orthogonal}$ in Fig. 7) with the two unpaired electrons in p-orbitals in a perpendicular arrangement. On the other hand, planarization to form $\mathbf{1}^{2-}_{planar}$ results in a much more stable product. This stabilization makes the reduction thermodynamically easier than expected from the purely electrostatic estimation.[13,23]

The ratio of the electron transfer rate constants k_{s1} and k_{s2} ($k_{s1}/k_{s2} \approx 2.5$–3; Table 4) indicates that the structural change of **1** may indeed occur during the second electron transfer. The 'inner reorganisation energy' related to this molecular rearrangement contributes to the activation barrier of the reduction to the dianion, and decreases k_{s2}.

To explain the effect of the substituents on the relative potential ordering for the reduction of the neutral dithiocarboxylates we consider the most likely electron distribution in the monoanions $\mathbf{1}^{\cdot -}$, which is given in a simple valence bond representation by the mesomeric structures in Fig. 8. Whereas in the structure on the left (unpaired electron occupying a p-orbital of a ring carbon atom) the cyclically delocalized π-electron system of the imidazole ring is distorted, the structure on the right (unpaired electron located in a p-orbital of the exocyclic C-atom) retains the π-electron sextet but suffers from an energetically unfavorable interaction between the alkyl groups and the coplanar p-orbital with the unpaired electron. While effects on the heterocyclic ring should be similar

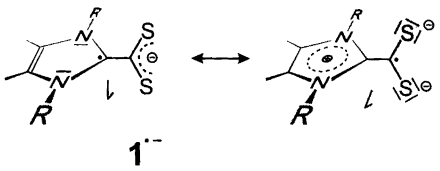

Fig. 8. Mesomeric valence bond structures for the monoanions $\mathbf{1}^{\cdot -}$.

for all three compounds, the interaction between the substituents and the p-orbital are expected to increase with the size of R. Thus, increasing steric strain is expected in the order methyl ($\mathbf{1a}^{\cdot -}$) < ethyl ($\mathbf{1b}^{\cdot -}$) < isopropyl ($\mathbf{1c}^{\cdot -}$) and consequently the energy of the monoanions increases. In the case of $\mathbf{1c}^{\cdot -}$ the monoanion energy becomes large enough to cause potential inversion, although at the same time the energy of $\mathbf{1c}^{2-}$ also increases (see $\overline{E^\circ}$ above).

The energetic relationship between the neutral starting compound and the mono- and di-anionic reduction products is shown in Fig. 9 on a relative Gibbs energy scale for all the investigated compounds. From the individual E°_i it is possible simply to calculate the $\Delta G^\circ_i = -nFE^\circ_i$ ($n=1$, $i=1,2$) for the reduction steps, referred to the fc/fc$^+$ redox couple, i.e. the Gibbs energy change for the equilibrium (3).

$$Ox + fc \rightleftharpoons Red + fc^+ \qquad (3)$$

In order to compare the three systems we normalize the ΔG°_i to the total $\Delta G^\circ = \Delta G^\circ_1 + \Delta G^\circ_2$ for the respective two-electron process. Furthermore, we set the Gibbs energy of the neutral dithiocarboxylates equal to zero. The resulting relative Gibbs energy G°_{rel} of the dianions is equal to unity. The G°_{rel} of the monoanions is below 0.5 for the methyl and the ethyl derivative. For the isopropyl compound with potential inversion, however, G°_{rel} is slightly above 0.5. Although the effect is rather small on the relative Gibbs energy scale, it causes dramatic changes in the cyclic voltammograms. This *relative*

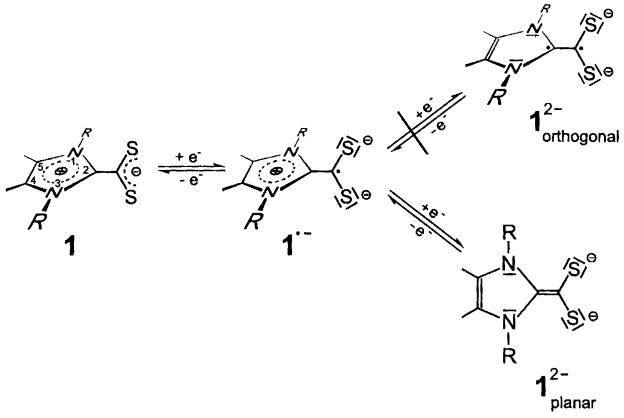

Fig. 7. Structural changes during stepwise two-electron reduction of **1** to orthogonal and planar dianions.

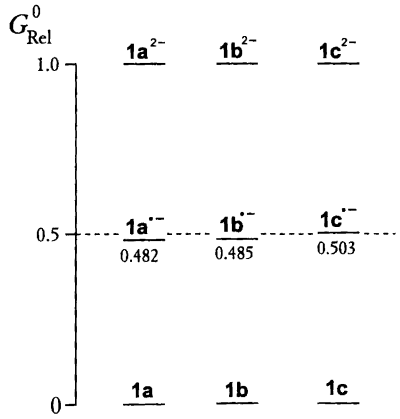

Fig. 9. Relative Gibbs free energies G°_{rel} (for definition see the text) of dithiocarboxylate mono- and di-anions.

increase of the monoanion energy is responsible for the occurrence of potential inversion in the present case.

Conclusions

The *N,N'*-dialkyl-4,5-dimethylimidazolium-2-dithiocarboxylates, which are reduced to the respective 1,1-dithiolate dianions at a GC electrode in THF at rather negative potentials, provide an example of the modulation by steric effect of the relative formal potentials of two-electron-transfer redox systems from compressed to inverted. A relatively simple valence bond model of the monoanions already suffices to explain the decrease in $|\Delta E^\circ|$ with increasing size of the substituents on the nitrogen atoms. The results presented in this paper confirm the relationship between structural changes and potential inversion.[23]

Experimental

Materials. The synthesis of the imidazolyl-2-ylidene–CS_2 adducts **1a–c** has been described before.[36] For electroanalytical experiments the raw materials were sublimed at 185 °C/5 × 10^{-2} mbar to remove electroactive impurities. Ferrocene (fc) was purchased from Aldrich.

Solvents and supporting electrolyte. Tetrabutylammonium hexafluorophosphate, NBu_4PF_6, was prepared from NBu_4Br and NH_4PF_6 as described before.[37] Purification of acetonitrile and dichloromethane followed procedures published recently.[24] Tetrahydrofuran (Aldrich, *purum*) was distilled over sodium–benzophenone and then passed through an Al_2O_3 column. The neutral Al_2O_3 had been activated for 5 h at 400 °C/5 × 10^{-5} mbar. All experiments with **1a–c** were performed in THF–0.2 M NBu_4PF_6. The electrolyte solutions were degassed before use by three freeze–pump–thaw cycles.

Electroanalytical experiments. Cyclic voltammograms and chronocoulograms were recorded with a BAS 100 B/W electrochemical workstation (Bioanalytical Systems, West Lafayette, IN, USA), controlled by a standard 80486 personal computer (control program version 2.0).

All electroanalytical experiments were carried out at room temperature under argon with a gas-tight full-glass three-electrode cell. The working electrode was a glassy carbon (GC) disk electrode (BAS), polished with α-Al_2O_3 (Buehler, 0.05 μm). The electroactive area of this electrode was determined from cyclic voltammograms, chronoampero- and chronocoulo-grams of fc in CH_2Cl_2–0.1 M NBu_4PF_6 to $A = (0.064 \pm 0.005)$ cm^2. For this calculation a value for the diffusion coefficient of fc in CH_2Cl_2, $D(\text{fc}) = 2.32 \times 10^{-5}$ cm^2 s^{-1} was taken from the literature.[38] The counter electrode was a platinum wire spiral (diameter of wire: 1 mm, diameter of spiral ≈7 mm).

In all experiments, a 'dual reference electrode system' as suggested by Garreau *et al.*[39] was used. An Ag/Ag^+ electrode (0.01 M $AgClO_4$–0.1 M NBu_4PF_6 in CH_3CN) served as the reference system and was separated by two glass frits from a Haber–Luggin capillary. A platinum wire (1 mm diameter) was immersed in the solution and connected through a 0.01 μF capacitor to this electrode.

All potentials in this paper are reported vs. an external fc/fc^+ standard.[40] The potential of the fc/fc^+ redox couple in the THF electrolyte was determined by five separate cyclic voltammetric experiments [E° (fc/fc^+) = (+0.176 ± 0.004) V vs. Ag/Ag^+]. The ferrocene/ferricinium couple behaves as a quasi-reversible redox system with a minimal peak potential difference of $\Delta E_p = (0.061 \pm 0.002)$ V ($v = 0.02$ or 0.05 V s^{-1}) in THF–0.2 M NBu_4PF_6.

Cyclic voltammetric and chronocoulometric curves are background- and *iR*-drop-corrected. Background curves were recorded before addition of substrate to the solution and subtracted afterwards by means of the BAS 100 B/W program. Since the automatic *iR*-compensation facility of the BAS 100 B/W instrument produced overcompensated current–potential curves, *iR*-compensation was performed manually. A series of cyclic voltammograms was recorded for all concentration–scan rate combinations with variation of the amount of compensation from undercompensation to beginning of oscillation. From this series the curve with maximum compensation but not showing oscillations or other distortions caused by overcompensation was selected. The same procedure was applied to the background curves.

Numerical simulations[41] were performed with the commercial program DigiSim[42] (BAS, version 2.1, FIFD algorithm, default numerical options), with the assumption of planar diffusion.

Acknowledgements. We thank the *Fonds der Chemischen Industrie*, Frankfurt am Main, Germany, for financial support.

References

1. Speiser, B., Tittel, C., Einholz, W. and Schäfer, R. *J. Chem. Soc., Dalton Trans.* (1999) 1741.
2. Marcus, R. A. *Angew. Chem. 105* (1993) 1161; *Angew. Chem., Int. Ed. Engl. 32* (1993) 1111.
3. Grampp, G. *Angew. Chem. 105* (1993) 724; *Angew. Chem., Int. Ed. Engl. 32* (1993) 691.
4. Miller, C. J. In: Rubinstein, I., Ed., *Physical Electrochemistry*, Marcel Dekker, New York 1995, p. 27.
5. Marcus, R. A. *Pure Appl. Chem. 69* (1997) 13.
6. Savéant, J.-M. *Adv. Phys. Org. Chem. 26* (1990) 1.
7. Speiser, B. *Angew. Chem. 108* (1996) 2623; *Angew. Chem., Int. Ed. Engl. 35* (1996) 2471.
8. Kurreck, H. and Huber, M. *Angew. Chem. 107* (1995) 929; *Angew. Chem., Int. Ed. Engl. 34* (1995) 849.
9. Deuchert, K. and Hünig, S. *Angew. Chem. 90* (1978) 927; *Angew. Chem., Intl. Ed. Engl. 17* (1978) 875.
10. Schwarz, H. A., Comstock, D., Yandell, J. K. and Dodson, R. W. *J. Phys. Chem. 78* (1974) 488.
11. Pierce, D. T. and Geiger, W. E. *J. Am. Chem. Soc. 111* (1989) 7636.
12. Pierce, D. T. and Geiger, W. E. *J. Am. Chem. Soc. 114* (1992) 6063.

13. Phelps, J. and Bard, A. J. *J. Electroanal. Chem. 68* (1976) 313.
14. Lowe, D. J. In: Müller, A., Rataijczak, H., Junge, W. and Diemann, E., Eds., *Electron and Proton Transfer in Chemistry and Biology*, Elsevier, Amsterdam, 1992, Vol. 78 of 'Studies in Physical and Theoretical Chemistry', p. 149.
15. Coucouvanis, D., Demadis, K. D., Malinak, S. M., Mosier, P. E., Tyson, M. A. and Laughlin, L. J. In: *ACS Symp. Ser., Transition Metal Sulfur Chemistry 117*, Am. Chem. Soc. 1996.
16. Tributsch, H. *J. Electroanal. Chem. 331* (1992) 783.
17. Zusman, L. D. and Beratan, D. N. *J. Chem. Phys. 105* (1996) 165.
18. Evans, D. H. *Acta Chem. Scand. 52* (1998) 194.
19. Zusman, L. D. and Beratan, D. N. *J. Phys. Chem. A 101* (1997) 4136.
20. Tributsch, H. and Pohlmann, L. *J. Electroanal. Chem. 438* (1997) 37.
21. Tributsch, H. and Pohlmann, L. *Science 279* (1998) 1891.
22. Heinze, J., Dietrich, M., Hinkelmann, K., Meerholz, K. and Rashwan, F. *Dechema-Monographien 112* (1988) 61.
23. Evans, D. H. and Hu, K. *J. Chem. Soc., Faraday Trans. 92* (1996) 3983.
24. Speiser, B., Würde, M. and Maichle-Mössmer, C. *Chem. Eur. J. 4* (1998) 222.
25. Tulyathan, B. and Geiger, W. E. *J. Am. Chem. Soc. 107* (1985) 5960.
26. Kuhn, N., Weyers, G., Dümmling, S. and Speiser, B. *Phosphorus, Sulphur, Silicon 128* (1997) 45.
27. Kuhn, N., Weyers, G. and Henkel, G. *J. Chem. Soc., Chem. Commun.* (1997) 627.
28. Kim, J. and Faulkner, L. R. *Anal. Chem. 56* (1984) 874.
29. Bard, A. J. and Faulkner, L. R. *Electrochemical Methods. Fundamentals and Applications*, Wiley, New York 1980, p. 204.
30. Anson, F. C. *Anal. Chem. 38* (1966) 54.
31. Ridgway, T. H., Van Duyne, R. P. and Reilley, C. N. *J. Electroanal. Chem. 34* (1972) 267.
32. Ryan, M. D. *J. Electrochem. Soc. 125* (1978) 547.
33. Hinkelmann, K. and Heinze, J. *Ber. Bunsenges. Phys. Chem. 91* (1987) 243.
34. Evans, D. H. *Chem. Rev. 90* (1990) 739.
35. Luo, W., Feldberg, S. W. and Rudolph, M. *J. Electroanal. Chem. 368* (1994) 109.
36. Kuhn, N., Bohnen, H. and Henkel, G. *Z. Naturforsch., Teil B 49* (1994) 1473.
37. Dümmling, S., Eichhorn, E., Schneider, S., Speiser, B. and Würde, M. *Curr. Sep. 15* (1996) 53.
38. Cooper, J. B. and Bond, A. M. *J. Electroanal. Chem. 315* (1991) 143.
39. Garreau, D., Savéant, J. M. and Binh, S. K. *J. Electroanal. Chem. 89* (1978) 427.
40. Gritzner, G. and Kůta, J. *Pure Appl. Chem. 56* (1984) 461.
41. Speiser, B. In: Bard, A. J. and Rubinstein, I., Eds., *Electroanalytical Chemistry*, Marcel Dekker, New York 1996, Vol. 19, p. 1.
42. Rudolph, M., Reddy, D. P. and Feldberg, S. W. *Anal. Chem. 66* (1994) 589A.

Received December 7, 1998.